Cooling history and differentiation of a thick North Mountain Basalt flow (Nova Scotia, Canada)

JD Greenough[1]*, and J Dostal[2]

[1] Department of Geology, Mount Allison University, Sackville, New Brunswick, Canada EOA 3CO
[2] Department of Geology, Saint Mary's University, Halifax, Nova Scotia, Canada B3H 3C3

Abstract. A thick (<175 m) North Mountain Basalt flow at McKay Head, Nova Scotia (Canada) shows ~25-cm-thick differentiated layers separated by ~130 cm of basalt in its upper 34 m. Upper layers (~5 m below the lava top) are highly vesicular whereas lower ones are pegmatitic and contain a thin (~2 cm) rhyolite band. The layering of the flow closely resembles that of some Hawaiian lava lakes. The vesicular basalts and mafic pegmatites are inferred to be liquid-rich segregations which drained into horizontal cracks that formed within a crystalline mush. The cracks resulted from a thermal contraction associated with cooling and shrinkage of the mush. Rhyolites were formed by in situ differentiation. Gas overpressures fractured the pegmatites and gas effervescence filter pressing forced silica-rich residual liquid from pegmatite interstices into the fractures creating bands. Chemical differences between the pegmatitic layers and early formed, highly differentiated upper vesicular layers may reflect a role for volatiles in the differentiation process along with crystal fractionation.

Introduction

Since the publication of drilling results on lava lakes in Hawaii (Helz 1980), it has been known that thick lava flows probably develop incipient layering as a result of in situ differentiation processes. Unfortunately, the precise three-dimensional relationships between rock types are often difficult to reconstruct from drill cores. In 1987 we discovered a thick layered tholeiitic lava flow with exemplary exposure in shoreline sections along the Bay of Fundy. Detailed examination of the layering revealed that individual layers are traceable for many tens of meters and that their character changes from mafic

pegmatites bearing thin rhyolite bands (~30 m below flow top) to vesicle-rich layers in the upper part of the flow (~5 m from the top). Since the cooling regime of lava flows is well understood as a result of studies in Hawaii (e.g. Marsh 1989), it seemed reasonable to hypothesize that the flow rocks might hold useful textural and chemical data for understanding differentiation processes in mafic intrusions as well as information on when these processes operate. We are not the first to appreciate the value of these thick North Mountain Basalt flows for deciphering the effects of differentiation mechanisms in mafic systems; this was noted much earlier by Bowen (1917) and Powers and Lane (1916).

The purpose of this paper is to present petrographic, mineral chemistry and bulk chemical data on the layered sequence of the upper flow of the North Mountain Basalt, to illustrate the internal variability generated within a single cooling unit, to consider the mechanisms which may have produced the observed differentiation, and to constrain the cooling history of the flow.

Geology and field description

The early Jurassic (190 Ma; Hayatsu 1979) North Mountain Basalt Formation consists of two thick lava flows (each typically 150–200 m thick), known as the lower and upper units, that are separated by thinner flows comprising the middle unit (thickness ~50 m) and overlain by thin flows of the overlying unit (thickness ~75 m) (Papezik et al. 1988; Greenough et al. 1989a). Mapping and Sr isotopic studies have shown that the two thick flows are traceable for over 230 km along the Bay of Fundy (Jones and Mossman 1988; Greenough et al. 1989a) and are the products of NE-trending fissure eruptions that transected the Fundy Basin during North Atlantic rifting (Fig. 1). The basalts are the typical high-Ti quartz-normative tholeiites of Weigand and Ragland (1970) with geochemical signatures suggesting the role of a crustal component in their genesis (Dostal and Dupuy 1984; Greenough et al. 1989b; Dostal and Greenough 1991).

* Present address: Department of Geological Sciences, University of British Columbia, Okanagan College, 1000 K.L.O. Road, Kelowna, British Columbia, Canada V1Y 4X8
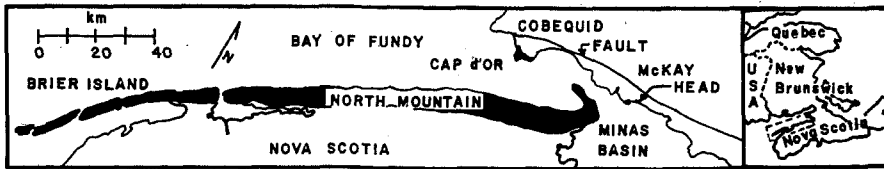
Fig. 1. Map showing the distribution of North Mountain Basalt and location of McKay Head
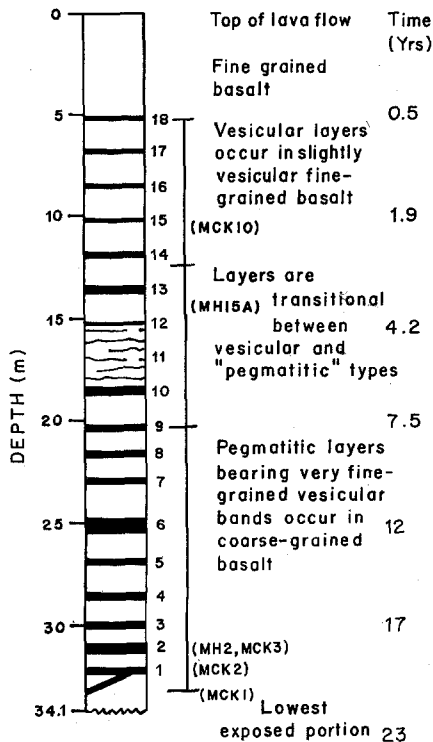

Fig. 2. Idealized stratigraphic section through the layered portion of the upper unit flow at McKay Head. *Broad dark lines* are proportional in width to pegmatitic layers (*bottom of section*) and vesicle-rich layers (*high in section*). Depth (*m*) below the top of the flow appears to the left with layer numbers, sample locations and summary rock descriptions on the right. Estimates of the time required for the advancing upper crust to reach various levels in the flow (according to methods of Marsh 1989) appear at the far right. Sample PA2 comes from an outcrop 11 km to the west of McKay Head but has a stratigraphic position similar to MCK10

Samples for this study come from exposures of the upper unit at McKay Head (Fig. 1). Although rocks bearing similar textural features occur at numerous localities around the Bay of Fundy, the section at McKay Head is, to our knowledge, the most complete and best illustrates the relationships between rock types. The basalt section consists of five thin lava flows that overlie the thick upper unit flow. The upper 34 m of the upper flow display somewhat regular layering (Figs. 2 and 3a).

In the lower portions of the layered section of the flow, pegmatitic gabbros between 6 and 56 cm in thickness (typically 25 cm across) are separated by coarse-grained basalt layers 80–180 cm thick (typically 130 cm, Fig. 2). In general, there is a fine-grained, sinuous, sharply defined, locally vesicular 'rhyolitic' band 1–4 cm wide in the middle of each pegmatitic layer (Fig. 3b). Pegmatitic layers at the bottom of the layered section (layers 1 and 2) display a variolitic texture with <15-cm-long sheaths of augite radiating from both sides of

the layer toward its centre. Individual fine-grained bands and the pegmatites that contain them are remarkably continuous and traceable for 50 m across the cliff face. The pegmatitic layers generally form sharp contacts with the coarse-grained basalts though locally they appear gradational (e.g. layer 2).

Above the 8th layer (Fig. 2), pegmatitic material disappears and is replaced by gabbro, but 1-4-cm-thick, highly vesicular bands persist that resist weathering and in outcrop resemble fine-grained bands in the underlying pegmatites. Moving up through this transition zone, the layers gradually change in character such that above layer 13 they are represented by 8-25-cm-thick vesicular basalt layers (Fig. 3c). Material between these vesicular basalt layers is finer-grained than the basalt between pegmatitic layers lower in the section. Layering becomes indistinct above layer 18 which occurs at least 5 m below the top of the flow. These vesicular layers were also recognized at an outcrop 11 km west of McKay Head. Field inspection shows that the flow is progressively more altered up-section with quartz, carbonate, celadonite and zeolites locally filling vesicles in the basalt. This phenomenon occurs regionally and is apparently due to the highly vesicular overlying flows acting as a fluid conduit (Greenough et al. 1989a).

Layering apparently resembling that at McKay Head has been reported from thick lava lakes in Hawaii (Helz 1980; Helz et al. 1989). Similar pegmatitic layers and lenses have also been reported from thick subaerial flows of other Mesozoic Eastern North America basalts (Emerson 1905; Horter 1990; Puffer and Horter 1991); Columbia River basalts (Puffer and Horter 1991); Proterozoic Keweenawan basalts of the Canadian Shield (Annells 1973); as well as various diabase sheets such as from the Palisades, New Jersey and the Karoo of southern Africa (Walker 1958).

Petrography and sampling information

Locations of geochemically analyzed samples appear in Fig. 2. Mineral and mesostasis analyses were carried out using a JEOL JXA-50A (Memorial University of Newfoundland) or JEOL JXA-8600 (University of Saskatchewan) wavelength-dispersive electron microprobe (selected analyses are given in Table 1).

The basalts from between layers (samples MCK1 and MH15A; Fig. 2) are composed of plagioclase (AN_{73-48}) and augite with minor amounts of Fe-Ti oxides and pigeonite and interstitial intergrowths of quartz and feldspar in the mesostasis. Augite has a limited range of compositions that average $Wo_{36} En_{44} Fe_{20}$ (Fig. 4). The mafic pegmatites (samples MCK2B, 2T, 3B, 3T and MH2P) are coarse-grained rocks, made up mainly of py-
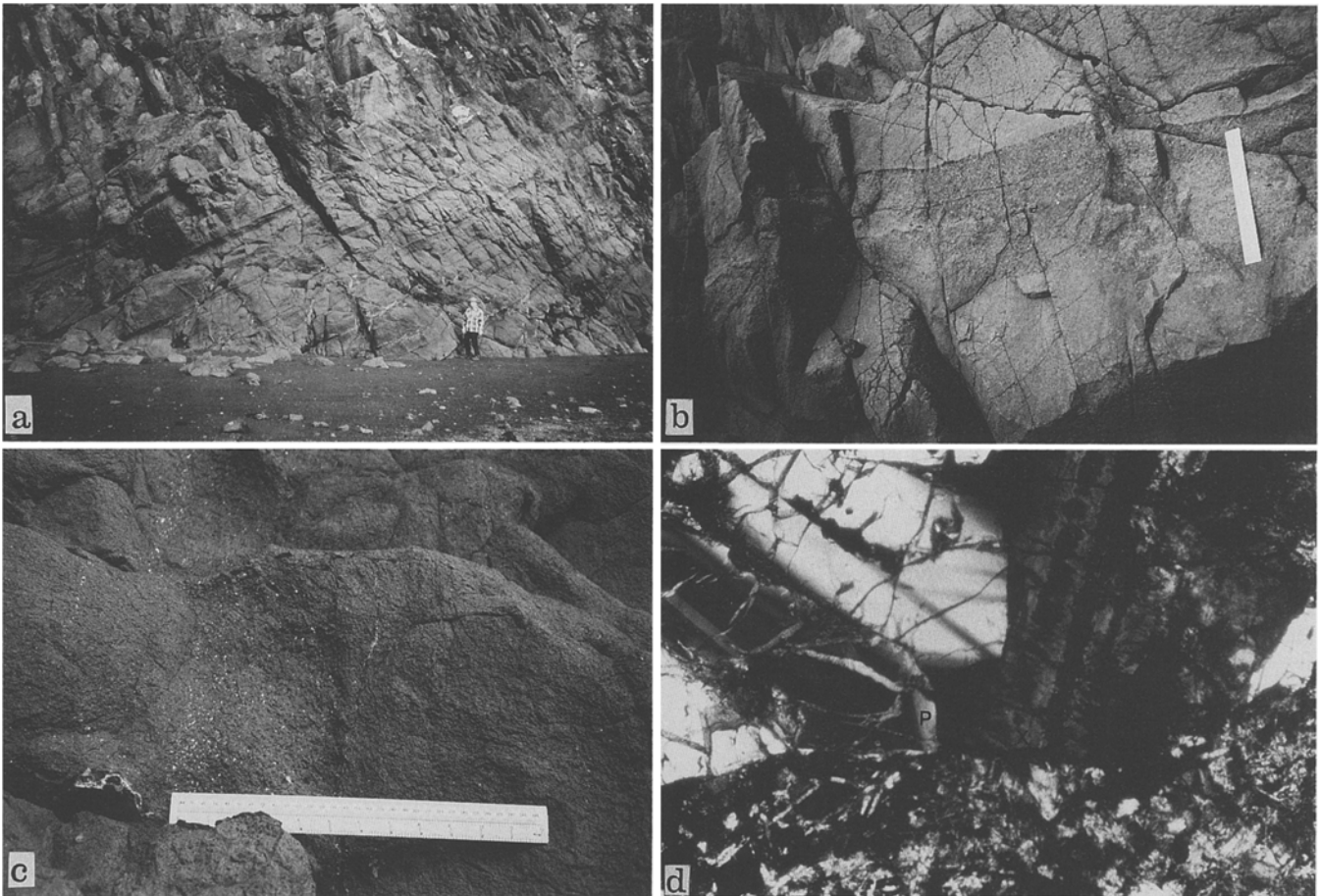
Fig. 3a–d. a Igneous layering in the thick flow at McKay Head. b Pegmatite layer (~No. 4, Fig. 2) with narrow and vuggy (vesicular) rhyolite band in the middle. Ends of the 30 cm rule closely coincide with the upper and lower boundaries of the pegmatite. c Photograph showing an easily weathered vesicular layer at McKay Head with 30 cm rule for scale. d Contact between rhyolite band (lower portion of photograph) and pegmatite. A long pyroxene crystal (X) and zoning (photograph taken under crossed nicols) in a plagioclase crystal (P) are truncated at the rhyolite band (photograph width = 3.25 mm)

roxene, zoned plagioclase (An$_{62-41}$), subordinate skeletal Fe-Ti oxides and a quartzo-feldspathic matrix that comprises 20% of the rocks and has a highly siliceous composition (Table 1). Augite has a mean composition (Wo$_{35}$ En$_{41}$ Fe$_{24}$) similar to that of the basalts, but the edges of some grains are Fe-rich (Fig. 4, Table 1). Locally the pyroxene is replaced by ferrorichterite (Table 1). Some pegmatites (e.g. MCK2B, 2T) show long (<15 cm) variolitic sheaths of augite crystals. Stilpnomelane (Table 1) forms interstitial microcrystalline masses which resemble glass (appears isotropic under crossed polars) and constitute up to 15–20% of the samples.

The fine-grained rhyolite bands (MCK2FG, 3FG and MH2FG) have sharp boundaries with the host pegmatites (Fig. 3d). The rhyolites display a granular texture with grains (<0.5 mm) of plagioclase (An$_{41-36}$) and K-feldspar intergrown with quartz. The other constituents of the rhyolites are accessory Fe-Ti oxides, minor pyroxene (~5%) and pockets of microcrystalline stilpnomelane (<5%). The Fe- and Ca-rich compositions of rhyolite pyroxenes are different from most other pyroxenes in the flow (Fig. 4; Table 1).

The vesicular layers (samples MCK10 and PA2) show an intersertal texture with a matrix (~25% excluding vesicle volume) of devitrified glass having a siliceous composition similar to that of the pegmatite mesostasis. Subhedral augite (~3.5 mm in size), zoned plagioclase (An$_{59-45}$) (<2.5 mm large) and Fe-Ti oxides are the other constituent phases. Compared with the basalt augites, the Fe/Mg ratios in the vesicular basalt pyroxenes are on average more Fe-rich (Wo$_{33}$ En$_{37}$ Fs$_{30}$), and display variable Ca (Fig. 4) and high Ti contents (~1% TiO$_2$, Table 1). Vesicles (up to 5 mm in diameter) comprise 30% of the rocks. Samples selected for analyses have unfilled vesicles or vesicles with thin (<3 mm) clay-mineral linings.

Geochemistry

Whole rock analyses appear in Table 2. Major elements and Rb, Sr, Ba, Zr, Nb, Y, V, Cr, Ni, Cu, Zn and Ga were determined by X-ray fluorescence while the rare-earth elements (REE), Sc, Co, Cr, Th and Hf were ana-

Table 1. Analyses of minerals and mesostasis

	Basalt			Vesicular layer	Rhyolite		Pegmatite		
	Plagioclase		Augite		Ferroaugite		Ferrori-chterite	Stilpno-melane[+]	Mesotasis[×]
	MH15A-3l	MH15A-4L	MH15A-4X	Pa2-9X	MCK2F-2X	MCK3B-4X	MCK2B-1A	MCK3T-ST	MCK2B-M
SiO_2 (%)	53.58	52.14	53.14	50.52	48.25	48.26	52.64	47.92	78.50
TiO_2			0.38	0.98	0.75	0.59	0.31	0.18	0.19
Al_2O_3	28.04	29.54	1.56	1.43	1.06	0.72	0.99	4.29	11.45
Cr_2O_3			0.15			0.02			
FeO^T	0.88	0.98	9.17	18.77	26.41	30.54	19.99	23.95	0.70
MnO			0.20	0.25	0.54	0.69	0.08	0.34	0.03
MgO			16.98	10.95	4.25	6.59	7.98	10.61	0.36
CaO	11.70	12.30	18.05	17.28	17.89	11.84	6.45	1.16	0.25
Na_2O	4.91	3.86	0.14	0.25	0.16	0.09	6.70	0.57	3.09
K_2O	0.36	0.27	0.01	0.00	0.02	0.00	0.00	0.63	5.41
P_2O_5								0.03	0.03
Total	99.47	99.09	99.63	100.43	99.33	99.34	95.14	89.68	100.01
Si	9.79	9.57	1.96	1.94	1.96	1.96	8.09	8.10	
Al	6.04	6.39	0.07	0.07	0.05	0.03	0.18	0.03	
Ti			0.01	0.03	0.03	0.02	0.04	0.82	
Cr			0.01	0.00	0.00	0.00	0.00		
Fe	0.13	0.15	0.28	0.60	0.90	1.04	2.57	3.38	
Mn			0.01	0.01	0.02	0.02	0.01	0.05	
Mg			0.93	0.63	0.26	0.40	1.83	2.67	
Ca	2.29	2.42	0.71	0.71	0.78	0.52	1.06	0.21	
Na	1.74	1.37	0.01	0.02	0.01	0.01	2.00	0.19	
K	0.08	0.06	0.00	0.00	0.00	0.00	0.00	0.14	

Mineral formulas calculated on basis of 32 oxygens for plagioclase, 6 oxygens for clinopyroxene, 23 oxygens for amphibole and 24 oxygens for stilpnomelane. FeO^T, total Fe as FeO. +, average of five analyses with beam 2 microns wide; x, average of five analyses with beam 10 microns wide
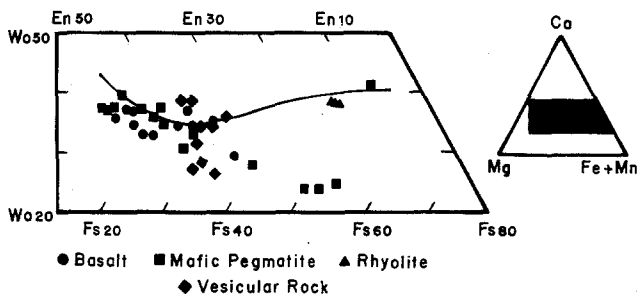

Fig. 4. Pyroxene quadrilateral showing pyxroxenes from the layered portion of the upper unit flow of North Mountain Basalt at McKay Head. For comparison the skaergaard crystallization trend is shown (from Brown 1957; Brown and Vincent 1963)

lyzed by the instrumental neutron activation technique at the Department of Geology of Saint Mary's University. Replicate analyses of standard rock AGV-1 indicate precision and accuracy for X-ray fluorescence trace element analyses of <4% for Rb, Sr, Zr, Nb, Y, V, Cr, Ni, Cu, Zn and Ga and <8% for Ba. Replicate analyses of standard rock W-1 indicate precision and accuracy better than 10% for the trace elements determined by neutron activation.

Each of the rock types (basalts, mafic pegmatites, rhyolites and vesicular layers) show distinctive chemical attributes. Basalts display intermediate Fe values (10–11

wt% total Fe as Fe_2O_3), slightly higher CaO (Fig. 5) and much higher Al_2O_3 (Table 2) and Cr concentrations (Fig. 6) compared to other rock types. The chondrite-normalized REE patterns display moderately sloping light REE and relatively flat heavy REE (Fig. 7). The compositions of these rocks are characteristic of North Mountain Basalt lavas that do not have significant accumulations of phenocrysts. The mafic pegmatites show high total Fe and lower Ca and Cr contents than the basalts (Fig. 5). Their high field strength (HFSE) and large ion lithophile (LILE) element concentrations including REE are similar to the basalts (Fig. 6) although the REE patterns of some samples show a negative Eu anomaly (Fig. 7). Individual pegmatites show distinct compositions (compare MgO and TiO_2 concentrations in MCK2 versus MCK3 samples) whereas samples from the bottom and top (e.g. MCK2B and MCK2T) of a particular pegmatite generally display smaller variations in composition.

The rhyolite bands can be distinguished on the basis of their high SiO_2 (up to 71wt% volatile free), K_2O (Fig. 5), Rb (up to 100 ppm, Fig. 6), Ba and Zr as well as low Fe_2O_3 (total Fe), TiO_2, CaO, MgO, Sr, Sc and V. REE concentrations are higher than in the other rock types (Table 2, Fig. 7) and the chondrite-normalized patterns, unlike the basalts and mafic pegmatites, do not flatten so much with the heavy REE. Compared to common rhyolitic and dacitic rocks (Ewart 1979), the bands have

Table 2. Whole-rock analyses of McKay Head rocks

	Basalts		Mafic	Pegmatites				Rhyolites			Vesicular basalts	
	MCK1	MH15A	MCK2B	MCK2T	MCK3B	MCK3T	MH2P	MCK2FG	MCK3FG	MH2FG	MCK10	PA2
SiO_2 (%)	51.00	53.15	51.20	52.10	52.70	51.80	53.70	69.30	68.90	64.58	51.20	55.40
TiO_2	1.40	1.35	1.52	1.44	1.88	1.76	1.88	0.72	0.64	0.94	2.52	2.51
Al_2O_3	14.60	14.49	10.60	12.30	12.80	13.00	12.53	10.60	10.40	11.17	11.70	11.54
$Fe_2O_3^T$	10.62	9.89	13.05	13.08	13.44	13.08	12.68	6.64	6.56	8.01	13.86	14.33
MnO	0.22	0.24	0.23	0.19	0.28	0.29	0.29	0.14	0.13	0.19	0.28	0.23
MgO	6.50	5.75	8.13	6.86	5.30	5.19	4.52	2.28	1.69	2.72	4.90	3.26
CaO	9.16	9.43	8.62	7.90	8.52	8.76	7.93	2.44	2.16	3.79	5.78	5.31
Na_2O	2.52	2.27	2.47	2.74	2.53	2.58	2.42	2.94	3.05	2.91	3.12	3.83
K_2O	0.82	0.83	0.81	0.88	0.95	0.91	1.28	2.67	2.78	2.48	1.76	2.31
P_2O_6	0.13	0.18	0.16	0.15	0.19	0.20	0.23	0.15	0.13	0.18	0.30	0.35
L.O.I.	2.30	1.60	2.52	2.94	1.55	0.17	1.90	1.66	2.41	2.70	3.82	0.40
Total	99.27	99.18	99.31	100.58	100.14	98.74	99.36	99.54	98.85	99.67	99.24	99.47
Mg #	0.55	0.54	0.55	0.51	0.44	0.44	0.41	0.41	0.34	0.40	0.41	0.31
Rb (ppm)	27	26	23	28	31	31	44	96	104	90	49	53
Sr	207	188	153	184	197	194	193	128	119	133	163	145
Ba	189	206	130	154	221	229	328	626	706	596	298	393
Th	2.80	3.10	2.40	2.78	3.24	3.32	4.32	11.3	12.2	10.0	5.96	6.29
Zr	118	130	106	118	137	138	177	398	431	355	255	263
Hf	3.10	3.10	2.70	3.01	3.47	3.32	4.44	10.6	11.4	9.22	6.32	6.62
Nb	11	14	13	13	13	14	16	25	26	21	19	24
Y	26	28	27	24	28	24	30	43	48	38	41	48
La	13.3	14.5	13.6	14.8	16.0	14.6	19.1	32.2	32.2	29.6	26.1	28.3
Ce	31.0	33.0	29.2	34.3	35.9	33.9	44.6	73.6	78.2	70.9	61.0	63.5
Sm	4.21	4.52	4.61	4.83	5.17	4.99	5.83	8.81	9.27	8.13	7.78	8.62
Eu	1.34	1.38	1.16	1.33	1.52	1.54	1.74	2.61	2.67	2.26	2.03	2.36
Tb	0.70	0.80	0.78	0.86	0.76	0.82	0.93	1.52	1.56	1.36	1.22	1.54
Yb	2.25	2.63	3.34	2.87	2.65	2.89	2.85	3.59	4.69	3.80	3.79	4.38
Lu	0.35	0.42	0.51	0.47	0.43	0.45	0.42	0.47	0.68	0.58	0.61	0.62
Sc	36	36	53	44	37	37	36	11	8.7	15	33	34
V	288	318	416	354	367	365	319	35	23	86	345	363
Cr	84	82	24	12	5.6	5.6	4	2.0	0.5	3.2	2.6	3.2
Co	52	47	69	62	59	59	61	58		58	52	47
Ni	34	19	36	27	10	14	13	1	0	3	6	23
Cu	170	184	126	145	185	214	215	280	343	304	36	291
Zn	64	86	66	54	78	86	80	64	33	44	73	103
Ga	16	21	14	15	18	18	17	17	17	13	20	19

Sample locations are given in Fig. 2. $Fe_2O_3^T$, total Fe as Fe_2O_3; B and T in sample numbers of pegmatites refer to material from below and above the rhyolite band; analyses of rhyolite bands correspond to analyzed mafic pegmatite samples; Mg #, $MgO/(MgO + FeO_t)$ in mol. %

high contents of Fe and Ti. However they resemble felsic rocks from bimodal basalt-rhyolite associations such as those from Iceland or Western Scotland (Ewart 1979).

The vesicular layers show the highest Fe_2O_3 (total Fe), TiO_2, Na_2O and P_2O_5 contents, and also plot between the rhyolite bands and mafic pegmatites on some variation diagrams (e.g. CaO and K_2O versus MgO, Fig. 5 and Rb, Sr and Ba versus Zr, Fig. 6). The rocks are strongly differentiated with Mg # ($MgO/MgO + FeO_t$ in mol.%) around 0.3-0.4 showing some compositional characteristics of tholeiitic ferrobasalts. Their light REE concentrations are lower than those of the rhyolite bands and the chondrite-normalized patterns are slightly flatter (Fig. 7).

Discussion

Effects of Alteration

The North Mountain Basalt, including the rocks at McKay Head, have been affected by zeolite facies metamorphism (Aumento 1966). At McKay Head the most obvious mineralogical effect of alteration is the formation of stilpnomelane. Elements known to be highly mobile during alteration of the basalt include Cu, Zn, and the alkali and alkali earth metals (Dostal and Dupuy 1984; Papezik et al. 1988; Greenough et al. 1989a). Nevertheless, Sr isotopic studies of the basalts have shown that most samples yield geochemical data suitable for petrogenetic interpretation, even where the alkali and alkali earth metals are concerned (Jones and Mossman 1988). We cannot rule out the possibility that some of the variability in, for example, vesicular layer Na_2O concentrations (Fig. 5) or Sr contents in the mafic pegma-

68

Fe$_2$O$_3$ 15 13 11 9 7

TiO$_2$ 2.25 1.25

CaO 7 4

Na$_2$O 3.8 3.4 3.0 2.6 2.2

K$_2$O 2.25 1.50

P$_2$O$_5$ 0.3 0.2

1   3   5   7   9

MgO

● Basalt
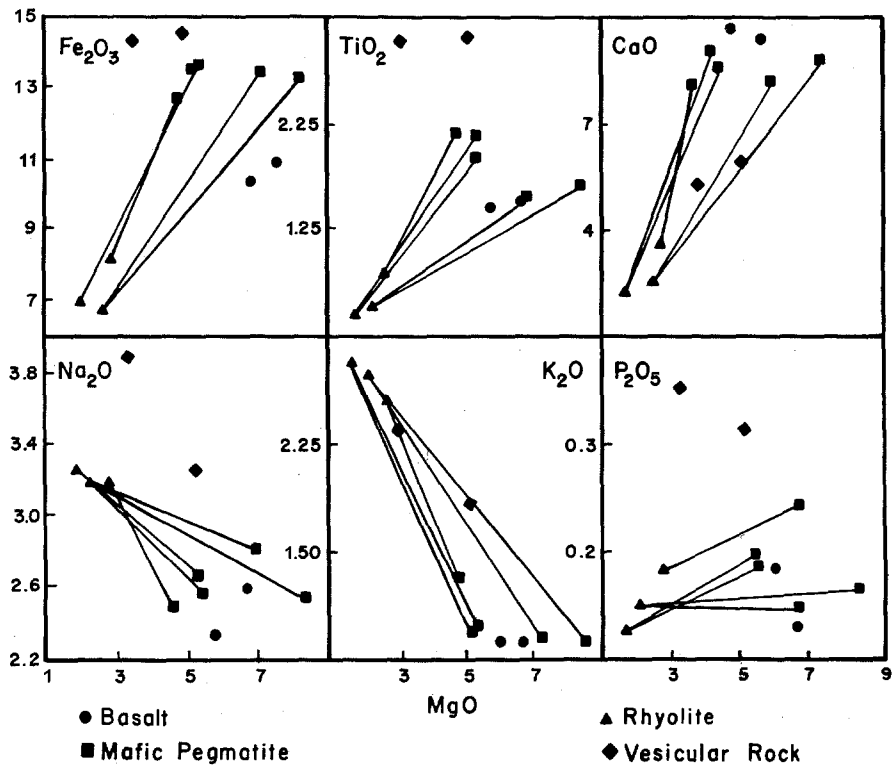■ Mafic Pegmatite
▲ Rhyolite
◆ Vesicular Rock

Fig. 5. Variation diagram showing selected major element oxides plotted against MgO (in wt% volatile free) for North Mountain rocks from McKay Head. Lines connect points representing the bottom, top and rhyolite band in the middle of a particular pegmatite (e.g. MCK2B, MCK2T, and MCK2FG)

Rb 100 80 60 40 20

Sr 200 175 150 125 100

Ba 640 480 320 160 0

Y 46 40 34 28 22

V 400 300 200 100 0

Cr 90 60 30 0

Hf 11 8 5 2

Th 12 9 6 3 0

Sc 50 30 10 0

125 225 325 425

Zr ⟶

● Basalt
▲ Rhyolite
■ Mafic Pegmatite
◆ Vesicular Rock

Fig. 6. Variation diagram showing trace elements plotted against Zr (in ppm) for North Mountain rocks from McKay Head
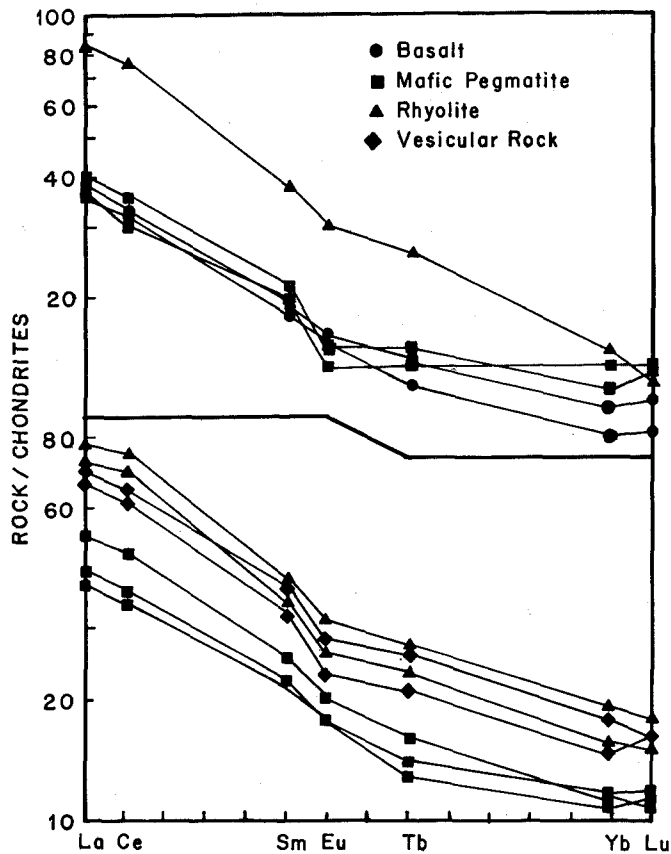
Fig. 7. Chondrite-normalized diagram showing REE patterns for the McKay Head rocks. Normalizing values are from Evensen et al. (1978)

connect these interstices with the rhyolite bands. These bands almost certainly were formed by in situ differentiation processes but the exact process or processes are not clear. Two mechanisms can be invoked to explain the origin of the rhyolite: liquid immiscibility and fractional crystallization.

1. Liquid immiscibility. The only definitive evidence for immiscibility is globules of one liquid (glass) inside another. Long and Wood (1986) documented the presence of two immiscible liquid silicate phases in similar basaltic flows. In those continental tholeiites, iron oxide-rich blebs are enclosed in basaltic glass. However, such evidence was not observed in the pegmatite samples. The immiscibility hypothesis can also be evaluated from the trace element distribution. Comparison of relative trace element abundances in the basalts, pegmatites and rhyolites (Table 3) gives qualitative information on element behaviour. For example, the average Zr concentration in the pegmatites is the same as in the basalts but one-third of that in the rhyolites. Thus, the Fe-rich liquid, retained in the pegmatites would have had a very low Zr content. This analysis indicates that Rb, Ba, Th and Zr partitioned into the Si-rich melt (rhyolite) and Sr and V entered the Fe-rich melt (mafic pegmatite) (or Fe-Ti oxides controlled V). Chromium, Ni and Sc partitioned into the Fe-rich melt or were controlled by pyroxene. Whether the REE, Y, Nb and Ga preferred the Fe-rich or Si-rich liquid cannot be determined.

These results can be compare with the partition coefficients measured in the synthetic systems (Watson 1976; Ryerson and Hess 1978) as done by various authors (e.g. Vogel and Wilband 1978; Eby 1980; Taylor et al. 1980). In the melting experiments, high-charge density cations (P, Ti, Zr, Th, Ta, Cr an the REE) were strongly enriched in the Fe-rich liquid, the alkali earth metals (Sr, Ba) showed slight to negligible enrichment in the Fe-rich liquid, and the alkali metals (K, Rb, Cs) were strongly enriched in the Si-rich liquid. The antithetic behaviour of Th, Zr, Hf and Ba relative to the experimental result indicates that McKay Head rhyolites were not formed through immiscibility.

2. Fractional crystallization. Normal fractionation processes should result in higher P_2O_5 concentrations in derivative rocks (Anderson and Gottfried 1971), providing apatite is not a liquidus phase. The low P_2O_5 content in the rhyolites is not consistent with a crystal fractionation origin for the rhyolite bands (means = 0.15% in rhyolite and 0.19% in pegmatite) unless the process involved fractionation of apatite. The other compositional differences between mafic rocks and rhyolites are qualitatively consistent with fractional crystallization although mass balance calculations failed to reproduce closely the rhyolite composition from the average basalt. Application of trace element modelling techniques in this case is poorly constrained because concentrations of the REE and HFSE are highly dependent on the amount of apatite fractionation which is difficult to assess. However, the element variations which are not readily consistent with a crystal fractionation model can be the

tites (Fig. 6) reflects the effects of alteration and the local formation of silpnomelane. However, in general, samples for each rock type plot coherently on variation diagrams suggesting that concentrations, for the most part, reflect primary values. Subsequent discussion treats Table 2 data as representative of primary compositions. Confidence in the conclusions must be tempered with this assumption.

Formation of Rhyolite Bands

Formation of the rhyolite bands through injection of a thin (~2 cm) layer of a foreign siliceous magma for horizontal distances greater than 50 m at regular vertical intervals is unlikely. Further, similar bands occur at various localities along North Mountain for a distance of 225 km from McKay Head. Possibly the flow assimilated sedimentary rocks at its base, but it is not probable that the rhyolite bands represent only assimilated material because they are regularly spaced and occur high in the flow.

The rhyolite material probably came from the pegmatites. Quartzo-feldspathic intergrowths filling large polygonal interstices in the pegmatites commonly display textures identical to those in the rhyolite bands. Locally, rhyolite-filled fractures penetrating the pegmatites

Table 3. Averaged data and modelling results

	Basalt[1]	Pegmatite[2]	Rhyolite[3]	Vesicular[4]	Model Vesicular[5]
SiO_2 (%)	54.10	53.93	71.62	55.61	55.10
TiO_2	1.43	1.71	0.70	2.62	2.47
Al_2O_3	15.11	12.64	10.88	12.13	13.06
FeO	9.59	12.30	6.15	13.23	13.75
MnO	0.24	0.26	0.14	0.27	0.36
MgO	6.36	6.61	2.06	4.26	5.53
CaO	9.66	8.77	2.38	5.79	5.34
Na_2O	2.49	2.68	3.10	3.63	2.67
K_2O	0.86	0.92	2.82	2.12	1.43
P_2O_5	0.16	0.18	0.15	0.34	0.29
Mg #	0.54	0.49		0.37	
Rb (ppm)	26	28	100	51	47
Sr	197	182	124	154	212
Ba	197	184	666	346	325
Th	3.0	2.9	12	6.1	5.2
Zr	124	125	415	259	224
Y	27	26	46	44	49
La	14	15	32	27	24
Sm	4.4	4.9	9.0	8.2	7.2
Eu	1.4	1.4	2.6	2.2	2.0
Yb	2.4	2.9	4.1	4.1	3.9
Sc	36	43	10	34	30
V	303	375	29	354	364
Cr	83	12	1	2.9	11
Co	50	62	76	50	76
Ni	26	22	1	14	15
Ga	18	16	17	20	21
Modelling data:					
Augite					0.433
Plagioclase					0.567
% Crystallization					45.3
R^2					4.69

Major elements recalculated to 100% volatile free. Total Fe as FeO. $Mg\#$, $MgO/(MgO + FeO_t)$ in mol.%. R^2, sum of squares residuals. The trace element abundances calculated using the partition coefficients of Frey et al. (1974) and Philpotts and Schnetzler (1970) for augite and plagioclase. *Numbers* beside augite and plagioclase give relative proportions of each phase removed.
1. Observed basalt = average of MCK1 and MH15A
2. Observed pegmatite = average of MCK2B, 2T, 3B and 3T
3. Observed rhyolite = average of MCK2FG and MCK3FG
4. Observed vesicular basalt = average of MCK10 and PA2
5. Vesicular layer composition modelled using mass-balance calculations. Augite = MH15A-4X; plagioclase = MH15A-4L (Table 1)

result of the movement of magmatic volatiles that may have altered the distribution of some elements in the rhyolite bands. Helz (1987) inferred that compositionally very similar segregations from Kilauea Iki lava lake formed by fractional crystallization. In fact the variation trends displayed by these segregations from the North Mountain Basalts fall on the liquid lines of descent of the Kilauea Iki rocks.

Segregation of Rhyolite Liquid

After formation, some of the rhyolite liquid segregated to form distinct bands. Broken pyroxene and plagioclase grains at the rhyolite interface show that the pegmatite crystals had formed prior to the rhyolite band. Propach

(1976) proposed that gas exsolution from interstitial magma can drive the liquid into low pressure fractures and/or voids. Anderson et al. (1984) mathematically demonstrated the process's feasibility and suggested that support for the process comes from the vesicularity of segregated material. Thus gas filter pressing provides a motive force for separation of the rhyolite. Thermal stresses from crystallization (~ 60 vol.%, corresponding with estimates of the volume of non-mesostasis material in the pegmatite) and contraction of the pegmatite could have contributed to fracturing. However, gas overpressure must have widened the fracture (now filled with rhyolite) which represents ~ 8 vol.% of the rock. Presumably the pegmatite fractured along the plane of greatest weakness.

Formation of Vesicular Layers

Vesicular layers near the top of the flow represent the most evolved mafic rocks observed. The rocks of the vesicular layers contain the highest Na_2O, P_2O_5, Fe_2O_3 and TiO_2 concentrations in the flow (Fig. 5). They are very similar chemically to rocks reported by Helz (1987) from Kilauea Iki lava lake. They have low Mg # (Table 2) indicating extensive fractionation. The high TiO_2 content of vesicular layer pyroxenes indicates that high TiO_2 concentrations were an intrinsic characteristic of the strongly evolved magma. Physicochemical processes possibly involved in the formation of the basaltic rocks of the vesicular layers include crystal settling, liquid immiscibility, convection-aided Soret diffusion, fractional crystallization with liquid segregation from a crystal mush (filter pressing) and possibly volatile transport of elements.

Numerous reasons why crystal settling is not a viable means for explaining layering and chemical separations in many mafic igneous bodies have been discussed in McBirney and Noyes (1979). In the case of the North Mountain Basalt at McKay Head, the settling model is not viable simply because there are no phenocryst accumulations. The high FeO (total Fe), TiO_2 and P_2O_5 concentrations in the vesicular rocks may lead to the suggestion that they represent an accumulation of Fe-rich liquid. However, there is no textural evidence for an immiscible origin.

Laboratory experiments designed to test for the effects of Soret diffusion show that a temperature differential of 200° C results in the separation of network-forming elements (Si, Al, Na, K) from network-disrupting elements on a scale similar in magnitude to that produced by crystal fractionation (Walker et al. 1981). Experiments on mid-ocean ridge basalts (MORB) indicate that Soret diffusion does not result in a Fe-enrichment differentiation trend and is thus probably not an important process affecting MORB (Walker and DeLong 1982, 1984; Elthon and Casey 1984). The applicability of these melting experiments to North Mountain Basalt (which has MORB affinities but high alkali metal concentrations, Dostal and Dupuy 1984) is not clear but given the significant Fe-enrichment in these basalts (Fig. 5), the effects of Soret diffusion are probably not important.

A model involving crystallization of the flow with filter segregation acting to produce the most evolved mafic rocks in the flow (i.e. the vesicular layers) can be evaluated using mass balance calculations (Bryan et al. 1969) and the Rayleigh fractionation law (e.g. Gast 1968) providing that an initial starting composition can be identified. Unfortunately unaltered 'contact' samples are not available. However, the similarity of basalt analyses in Table 2 with all samples below the layered portion of the flow (Greenough et al. 1989a) and a lack of cumulus texture suggests that an average of Table 2 basalt analyses provides an approximation of the undifferentiated flow composition. Basalt pyroxene and plagioclase analyses were used in the mass balance calculations and these results (phase proportions and percentage crystalli-

zation) were utilized in trace element modelling. Results are given in Table 3. The fit to the least squares mixing model is good considering the uncertainties involved in the measurements/sampling and averaging. The exceptions are alkalis which are enriched in the vesicular basalts over the abundances predicted by crystal fractionation. The alkali excesses are consistent with the role of the volatile components.

The basaltic rocks of the vesicular layer represent an advanced stage of crystallization of the basaltic magma ($\sim 50\%$, Table 3). Such a highly differentiated melt was probably saturated or supersaturated in volatiles. The vesicular character of these rocks suggests that volatile constituents were concentrated in the vesicular layers of the flow at McKay Head and their composition may have been affected by the accumulation of volatiles. The low solubility of elements such as Na in a high temperature gaseous phase (Holland and Malinin 1979) suggests that if volatile movement were an important process, metals were moved in the form of volatile complexes dissolved in the magma. Movement of these complexes implies a role for convection within the flow.

Formation of Layering

Layering found at McKay Head clearly resembles that in some of the thicker Hawaiian lava lakes (Helz 1980; Helz 1987 and references therein). For example, in Kilauea Iki lava lake, distinct, horizontally continuous (< 100 m) layers occur between depths of 20–52 m with spacings of between 1.7 and 2.8 m and thicknesses of 0.1–1.5 m. Wright and Okamura (1977) suggested that the horizontal layers may have formed as segregation (filter pressing) infillings of fractures when the upper crust became supported by crater walls. However, the thickness of some layers makes them difficult to explain by filter pressing and the layers are better developed away from the crater walls, casting doubt on the crust suspension model (Helz 1980). At McKay Head (and elsewhere around the Bay of Fundy) the regular spacing of layers is difficult to explain by this hypothesis, and there are not crater walls.

The formation of various types of layering in mafic intrusions has been discussed in detail by McBirney and Noyes (1979). The process of 'magmatic sedimentation' can be eliminated in the case of the flow at McKay Head because cumulus textures are not observed. Similarily, the nucleation-diffusion model explains fine-scale (< 1 m) oscillatory layering in intrusions but not the metre-scale intermittent layering at McKay Head where pegmatitic and vesicular layers rich in felsic components are separated by unlayered homogeneous rocks rich in mafic minerals. This latter type of layering has been attributed to the formation of convection cells as a result of opposing density gradients caused by thermal and compositional variations within magma chambers (McBirney and Noyes 1979; Huppert and Sparks 1980; McBirney 1985). However, double diffusive convection appears unlikely in the case of the North Mountain Basalts because melt density must decrease with decreasing

temperature, an unlikely condition when plagioclase is a major liquidus phase.

Our preferred model for the origin of layering in the North Mountain Basalts is similar to that discussed by Helz et al. (1989) and Marsh (1990) for Hawaiian lava lakes. Drilling at Kilauea Iki shows that the layers form in a crystal mush having sufficient rigidity to tear. This produces the relatively sharp boundaries such as observed between basalts and pegmatites at McKay Head (Fig. 3b). Tearing is presumably induced by thermal contraction and Marsh suggests that thick continuous layers may result from partial foundering of the mush into the underlying magma. As the horizontal fracture opens, interstitial liquid is siphoned from the adjacent mush.

Cooling History

The rate of cooling and solidification of the lava flow can be estimated from the rate of upper crust growth using the Stefan model (Marsh 1989) which duplicates the observed cooling history of Hawaiian lava lakes. The model places constraints on the time required for the formation of various rock types and by inference on the period when processes responsible for their formation were active. Times required for upper crust growth to various depths in the flow at McKay Head (Fig. 2) were calculated following Marsh (1989). The uppermost vesicular layers formed after approximately six months' cooling with the lowermost layers representing 25 years of cooling.

An important problem is why the earliest formed layers (vesicular layers) are chemically different from the lowermost layers (mafic pegmatites). The pegmatites (plus rhyolite) are not chemically as differentiated (e.g. lower Fe and Ti) as vesicular layers (Fig. 5). It has been pointed out that the composition of the uppermost layers cannot entirely be explained by crystal fractionation. Two possible explanations for these compositional variations include movement of volatiles via early convection in the magma and early movement of volatile-rich vesicle plumes as described by Helz et al. (1989). The possibility of large-scale convective overturn of the entire magma lens cannot be ruled out but is not expected to be vigorous (Marsh 1990). Vesicle plumes are preserved near the base of North Mountain basalt flows, thus this is proably the most plausible explanation. Both these mechanisms for volatile movement are expected to be most vigorous early in the cooling history of the flow. Thus the distinct composition of the uppermost layers, their time of formation and vesicular appearance, argue for some connection between the movement of volatile constituens and differentiation.

Textural differences between layers reflect changes in the cooling regime with time and depth. Large percentages of glass in the vesicular layers indicate supercooling whereas the curved and branching pyroxene textures of the pegmatites suggest significant though lesser amounts of supercooling (Lofgren 1974; Lofgren and Donaldson 1975). Because the rate of advance of the crystallization front is inversely proportional to the square root of time after emplacement (Jaeger 1968), these differences indicate that as the rate of advance decreased with depth, so too did the amount of supercooling in the differentiated layers.

Summary and conclusion

Thick lava flows such as at McKay Head contain chemical and textural features that may be useful for understanding differentiation of mafic magmas in general. The flow is layered with upper differentiates (~ 5 m below top) consisting of highly vesicular basalt and lower layers (below 20 m) composed of mafic pegmatite bearing a thin rhyolite band. All layers are inferred to be liquid-rich segregations drained into horizontal cracks that form at regular intervals (1.5 m) as mush grows down into the magma lens. The horizontal cracks are presumably induced by cooling and contraction of the crystal mush. The position of the vesicular layers in the flow shows that the most chemically differentiated mafic rocks formed only months after extrusion. The chemical composition of these rocks can largely be explained by simple crystal fractionation processes, but in detail some elements (e.g. alkali metals) appear to require another process. The highly vesicular nature, time of formation, and anomalous composition of these rocks suggests a role for the movement of volatile complexes during differentiation. Mafic pegmatites below the vesicular layers contain textures indicative of a decrease in the amount of supercooling as cooling rates decreased. Rhyolite bands in the middle of the pegmatites formed during a second stage of thermal fracturing with liquid squeezed from pegmatite interstices via gas filter pressing processes.

References

Anderson AT, Gottfried D (1971) Contrasting behaviour of P, Ti and Nb in a differentiated high-alumina olivine-tholeiite and a calc-alkaline andesite suite. Geol Soc Am Bull 82:1929–1942

Anderson AT, Swihart GH, Artioli G, Geiger CA (1984) Segregation vesicles, gas filter-pressing, and igneous differentiation. J Geol 92:55–72

Annells RN (1973) Proterozoic flood basalts of eastern Lake Superior: The Keweenawan volcanic rocks of the Mamainse Point area, Ontario. Geol Surv Can Pap 72-10:51

Aumento F (1966) Zeolite minerals, Nova Scotia. In: Geology of parts of the Atlantic Provinces. Geol Assoc Can Mineral Assoc Can Guidebook, pp 71–77

Bowen NL (1917) Discussion of 'Magmatic differentiation in effusive rocks'. Trans Am Inst Mining Eng 54:455–457

Brown GM (1957) Pyroxenes from the early and middle stages of fractionation of the Skaergaard intrusion, East Greenland. Mineral Mag 31:511–543

Brown GM, Vincent EA (1963) Pyroxenes from the late stages of fractionation of the Skaergaard intrusion. J Petrol 4:175–197

Bryan WB, Finger LW, Chayes F (1969) Estimating proportions in petrographic mixing equations by least-squares approximation. Science 163:926–927

Dostal J, Dupuy C (1984) Geochemistry of North Mountain basalt (Nova Scotia, Canada). Chem Geol 45:245–261

Dostal J, Greenough JD (1992) Geochemistry and petrogenesis of the Early Mesozoic North Mountain basalts of Nova Scotia, Canada. In: Puffer JH, Ragland P (eds) Mesozoic magmatism in eastern North America. Geol Soc Am Spec Pap (in press)

Eby GN (1980) Minor and trace element partitioning between immiscible ocelli-matrix pairs from lamprophyre dikes and sills, Monteregian Hills petrographic province, Quebec. Contrib Mineral Petrol 75:269–278

Elthon D, Casey JF (1984) Comment on 'Soret separation of mid-ocean ridge basalt magma' by D Walker and SE Delong. Contrib Mineral Petrol 85:197–202

Emerson BK (1905) Plumose diabase and palagonite from the Holyoka trap sheet. Geol Soc Am Bull 16:91–130

Evensen NM, Hamilton PJ, O'Nions RK (1978) Rare-earth abundances in chondritic meteorites. Geochim Cosmochim Acta 42:1199–1212

Ewart A (1979) A review of the mineralogy and chemistry of Tertiary-Recent dacitic, latitic, rhyolitic and related salic volcanic rocks. In: Barker F (ed) Trondhjemites, dacites and related rocks. Elsevier, Amsterdam, 13–121

Frey FA, Bryan WB, Thompson G (1974) Atlantic ocean floor: Geochemistry and petrology of basalts from Legs 2 and 3 of the Dep Sea Drilling Project. J Geophys Res 79:5507–5527

Gast PW (1968) Trace-element fractionation and the origin of tholeiitic and alkaline magma types. Geochim Cosmochim Acta 32:1057–1086

Greenough JD, Jones LM, Mossman D (1989a) Petrochemical and stratigraphic aspects of North Mountain basalt from the north shore of the Bay of Fundy, Nova Scotia, Canada. Can J Earth Sci 26:1701–1707

Greenough JD, Jones LM, Mossman D (1989b) The Sr isotopic composition of early Jurassic mafic rocks of Atlantic Canada: implications for assimilation and injection mechanisms affecting mafic dykes. Chem Geol 80:17–26

Hayatsu A (1979) K-r isochron age of the North Mountain basalt, Nova Scotia. Can J Earth Sci 16:973–975

Helz RT (1980) Crystallization history of Kilauea Iki lava lake as seen in drill core recovered in 1967–1979. Bull Volcanol 43:675–701

Helz RT (1987) Differentiation behavior of Kilauea Iki lava lake, Kilauea Volcano, Hawaii: An overview of past and current work. In: Mysen BO (ed) Magmatic processes, physiochemical principles. Geochemical Soc Spec Pub 1:241–258

Helz RT, Kirschenbaum H, Mainenko JW (1989) Diapiric transfer of melt in Kilauea Iki lava lake, Hawaii: a quick, efficient process of igneous differentiation. Geol Soc Bull 101:578–594

Holland HD, Malinin SD (1979) The solubility and occurrence of non-ore minerals. In: Barnes HL (ed), Geochemistry of hydrothermal ore deposits. John Wiley & Sons, New York, pp 461–508

Horter DL (1990) The nature and origin of pegmatite zones in the Lolo Flow, Columbia River Basalt group, Pasco Basin, Washington. M Sc Thesis, Rutgers University, Newark, New Jersey, 107 pp

Huppert HE, Sparks RSJ (1980) The fluid dynamics of a basaltic magma chamber replenished by influx of hot dense ultrabasic magma. Contrib Mineral Petrol 75:279–289

Jaeger JC (1968) Cooling and solidification of igneous rocks. In: Hess HH, Poldervaart A (eds) Basalts. Wiley Interscience, New York:503–536

Jones LM, Mossman DJ (1988) The isotopic composition of strontium and the source of the Early Jurassic North Mountain basalt, Nova Scotia. Can J Earth Sci 25:942–944

Lofgren G (1974) An experimental study of plagioclase crystal morphology: isothermal crystallization. Am J Sci 274:243–273

Lofgren GE, Donaldson CH (1975) Curved and branching crystals and differentiation in comb-layered rocks. Contrib Mineral Petrol 49:309–319

Long PE, Wood BJ (1986) Structures, textures and cooling histories of Columbia River basalt flows. Geol Soc Am Bull 97:1144–1155

Marsh BD (1989) On convective style and vigor in sheet-like magma chambers. J Petrol 30:479–530

Marsh BD (1990) Igneous processes in sills. In: Pacific Rim 90 Congress, Proceedings, Australian Institute of Mining and Metallurgy, 5 p

McBirney AR (1985) Further considerations of double-diffusive stratification and layering in the Skaergaard intrusion. J Petrol 26:993–1001

McBirney AR, Noyes RM (1979) Crystallization and layering of the Skaergaard intrusion. J Petrol 20:487–554

Papezik VS, Greenough JD, Colwell J, Mallinson T (1988) North Mountain basalt from Digby, Nova Scotia: Models for a fissure eruption from stratigraphy and petrochemistry. Can J Earth Sci 25:74–83

Philpotts AR, Schnetzler CC (1970) Phenocryst-matrix partition coefficients for K, Rb, Sr and Ba with applications to anorthosite and basalt genesis. Geochim Cosmochim Acta 34:307–322

Powers S, Lane AC (1916) Magmatic differentiation in effusive rocks. Trans Am Inst Mining Eng 54:442–455

Propach G (1976) Models of filter differentiation. Lithos 9:203–209

Puffer JH, Horter DL (1991) Basaltic pegmatites of the Lolo Basalt, Washington and the Watchung Basalts, New Jersey. 26th Annual Northeastern Section, Geol Soc Am Abstracts with Programs 23:118

Ryerson FJ, Hess PC (1978) Implications of liquid-liquid distribution coefficients to mineral-liquid partitioning. Geochim Cosmochim Acta 42:921–932

Taylor TR, Vogel TA, Wilband JT (1980) The composite dikes at Mount Desert Island, Maine: an example of coexisting acidic and basic magmas. J Geol 88:433–444

Vogel TA, Wilband JT (1978) Coexisting acidic and basic melts: geochemistry of a composite dike. J Geol 86:353–371

Walker F (1958) The pegmatitic differentiates of basic sheets. Am J Sci 251:41–60

Walker D, DeLong SE (1982) Soret separation of mid-ocean ridge basaltic magma. Contrib Mineral Petrol 79:231–240

Walker D, DeLong SE (1984) A small Soret effect in spreading centre gabbros. Contrib Mineral Petrol 85:203–208

Walker D, Lesher CE, Hays JF (1981) Soret separation of lunar liquid. Lunar Planet Sci Abstr 12:1130–1132

Watson EB (1976) Two-liquid partition coefficients: Experimental data and geochemical implications. Geochim Cosmochim Acta 56:119–134

Weigand PW, Ragland PC (1970) Geochemistry of Mesozoic dolerite dikes form eastern North America. Contrib Mineral Petrol 29:195–214

Wright TL, Okamura RT (1977) Cooling and crystallization of tholeiitic basalt, 1965 Makaopuhi Lava Lake, Hawaii. US Geol Surv Prof Pap 1004:78